Computing and Informatics, Vol. 43, 2024, 1483–1515, doi: 10.31577/cai_2024_6_1483

TWO-STAGE TRADING MECHANISM IN ENABLING THE DESIGN AND OPTIMIZATION OF FLEXIBLE RESOURCES INTERACTION IN SMART GRID

Yipeng Chen, Huaqiang Li, Yang Liu*, Shuning Wu, Xuan Li

College of Electrical Engineering
Key Laboratory of Intelligent Electric Power Grid of Sichuan Province
Sichuan University
Chengdu 610065, China
e-mail: Yang.Liu@scu.edu.cn

Man Qi

School of Engineering, Technology and Design
Canterbury Christ Church University
Canterbury, CT1 1QU, U.K.

Abstract. Currently, renewable energy sources (RES) have been widely deployed in the smart grid, especially in the active distribution network (ADN). However, the inherent uncertainty of the renewable energy output significantly impacts the economy of the ADN operation. It is suggested that the utilization of flexible resources (FR) can effectively even out the uncertainty of RES. Nevertheless, the non-marketization of FR may prevent the emerging park-level integrated energy systems (PIES), important entities in ADN, from sufficiently offering their potential flexibilities. Therefore, this paper presents a two-stage local flexibility trading mechanism for motivating multi-PIESs to provide their flexible resources (PFR) to improve the operational flexibility of ADN. The first stage determines the dispatching plan of ADN according to the day-ahead forecasted values of RES. The second stage enables the multi-PIESs to trade their PFR with ADN to adjust the day-ahead dispatching plan in real-time to correct the forecasted errors of RES. In terms of implementing the two stages, firstly, the capacity of PFR with involving the adjustable tie line power of PIES is quantified using an optimization-based as-

* Corresponding author

sessment model. Secondly, based on the change of the operation cost before and after the sale of PFR, a pricing model of PFR is established. And then, to determine the trading amount of PFR, a real-time ADN economic dispatching model with the network constraints is further constructed, which aims at minimizing the comprehensive operation cost. Afterwards, a marginal-based method is employed to obtain the clearing price of PFR. Finally, to ensure the feasibility of the trading results and to provide the accurate dispatching strategies for the PFR trading in next time interval, a rolling dispatch for the multi-PIESs is carried out. Case studies demonstrate that the presented flexibility trading mechanism significantly reduces the power curtailment of ADN, the operation costs of ADN and the multi-PIESs.

Keywords: Renewable energy, active distribution network, park-level integrated energy system, flexible resources, trading mechanism, operational flexibility

1 INTRODUCTION

Due to the energy depletion and the environmental issues, renewable energy, such as solar power and wind power, are increasingly deployed in the modern smart grid [1]. As an important part of the smart grid, it has been admitted that ADN is one of the most convenient ways to connect the distributed and small-scale RES at the local level [2]. However, the power output of RES can be severely impacted by quite a few external factors including the locations, the weather, and so on [3]. Therefore, the output of RES is frequently associated with uncertainty, which results in the difficulties of implementing the accurate prediction [4]. Consequently, the uncertainty of RES may lead to the real-time power imbalance, which significantly affects the economic operation of ADN [5]. Recently, numbers of researches have pointed out that improving the operational flexibility of ADN, which refers to the capability to accommodate the uncertain RES without serious power curtailment, could be an effective approach [6] to handle the RES uncertainty.

Alhelou et al. [7] investigated the flexibility from a perspective of the substation. An FR model of delineating the flexibility that the substation can provide has been established. However, supplying flexibility using the substation may encounter the price spike and the severe power loss problems in the upper grid [8]. Therefore, several studies focused on analyzing the flexibility of the distributed energy resources (DERs), such as the combined heat and power unit (CHP) [9], the gas boiler (GB) [10] and the electrical energy storage (EES) [11]. These DERs can be aggregated and managed by PIES which is also an important participator of ADN. The operator of PIES (PO) can flexibly dispatch the internal DERs to change the tie line power to implement the power exchange between PIES and ADN [12]. This feature enables PO to provide flexibility for the operator of ADN (DSO). Although the FR models of DERs have been widely studied [13], few researches have regarded the adjustable tie line power as an FR and quantitively analyzed its flexibility. There-

fore, to exploit the flexible adjustment capability contained in the tie line power can significantly expand the reserve of the local FR. Meanwhile, it provides an overall system perspective to analyze the total flexibility contained in PIES.

Li and Xu [14] pointed out that a system-wide optimal dispatching method for the multi-PIESs is able to improve the operational flexibility of ADN. Cheng et al. [15] further investigated the adjustment capability of PIES to join the operation of ADN, in which the authors demonstrated the effectiveness of the presented coordinated operation strategy. Additionally, to deal with the uncertainty of RES, Liu et al. [16] reported that based on the robust optimization method the operation cost of the system could be significantly reduced with involving the interaction among the multi-PIESs and ADN. However, in the traditional coordinated operations, PIESs are only the price-takers without actively participating in the market transaction, which reduces their activeness to join the operation of ADN. Therefore, Ostovar et al. [17] presented a decentralized pool strategy for PIESs to integrate with ADN using a trading mechanism, in which multi-PIESs are developed as the price-makers to find the optimal bidding strategy. However, there is a lack of research of involving the flexibility transaction in the coordinated operation strategies. Therefore, to motivate the multi-PIESs to actively provide flexibility, designing specialized trading mechanism makes great sense.

Recently, it is suggested that the local flexibility markets (LFM) can further provide the opportunities to trade flexibility among DSO and other participants (e.g., individual DERs or aggregators) in an economically efficient way [18]. However, the participation of the individual DERs or prosumers in LFM may encounter two issues:

1. The benefits of the individual DERs or prosumers cannot be guaranteed due to their limited negotiating power;
2. The computational intensity for the market clearing may sharply increase due to the large number of DERs [18].

Therefore, to employ the aggregators to gather and manage various DERs and prosumers (producer and consumer) in LFM has been proved to be an effective way to solve these issues [19, 20]. Olivella-Rosell et al. [19] designed an LFM trading mechanism operated by the residential aggregators to provide multiple flexibility services. Torbaghan et al. [20] also presented an LFM trading mechanism which focuses on maximizing the social welfare. Furthermore, to improve the trading profits and ensure the feasibility of the trading results, researches [21] also suggested that the accuracy of the dispatching strategy is quite necessary. Li et al. [22] presented a transactive energy trading platform with computing the optimal power flow to realize the real-time update of the dispatching strategies, so that the reliability and security of the system operation could be guaranteed. However, in their research the impact of the dispatching results on the energy trading process in next time interval is ignored, which may increase the transaction risk. In this regard, Lin et al. [23] pointed out that the rolling optimization adjusts the dispatching strategies in real

time, which effectively solves the inaccuracy of the day-ahead dispatching plans. Furthermore, Cao et al. [24] presented a two-stage energy generation schedule market rolling optimization framework. However, the current dispatching researches only focused on serving the traditional energy market. As a result, in terms of serving LFM, a novel rolling optimization strategy is quite essential.

Therefore, this paper presents a two-stage local flexibility trading mechanism aiming at motivating the multi-PIESs to provide their PFR to help improve the operational flexibility of ADN with involving the uncertainty of RES. The main contributions are as follows:

- A two-stage local flexibility trading mechanism of which DSO and the multi-PIESs are respectively the flexibility demander and the suppliers is developed. The first stage determines the dispatching plan of ADN based on the day-ahead forecasted values of RES and the power purchasing plans of the multi-PIESs. The second stage allows the multi-PIESs to trade PFR with DSO to adjust the day-ahead dispatching plan to correct the gaps between the forecasted values and the actual values of RES.
- With the consideration of the dynamic adjustment ability of the tie line power, an optimization-based model is established to assess the capacity of PFR. Furthermore, based on the changes of the operation cost before and after the sale of PFR, a pricing model of PFR is constructed.
- A real-time ADN economic dispatch with the network constraints is carried out by DSO to determine the trading amount of PFR. And then, a marginal-based method is adopted to obtain the market clearing price of PFR.
- A rolling optimization model with involving the real-time trading results of PFR is constructed to obtain the accurate dispatching strategies of PIESs, which serve as the reference values for PFR trading in next time interval.

The rest of this paper is organized as: Section 2 presents the market participants and the transaction process; Section 3 establishes the day-ahead dispatching models of the multi-PIESs and ADN; Section 4 introduces the detailed mathematical models for the PFR capacity assessment and its pricing; Section 5 constructs the real-time optimization model of ADN and presents the market clearing method of PFR; Section 6 presents the rolling optimization method for the multi-PIESs; Section 7 introduces the model processing and the solution method; Section 8 shows and discusses the case studies; Section 9 concludes this paper.

2 FLEXIBILITY TRADING MECHANISM

As renewable energy cannot be accurately forecasted in advance, forecasted errors generally result in power imbalances during the real-time operations. Consequently, load shedding and renewable power curtailment are required to maintain the operation security of ADN. To avoid serious power curtailment, this paper presents

a two-stage flexibility trading mechanism, which motivates the multi-PIESs to provide their PFR to improve the operational flexibility of ADN. The architecture of the presented flexibility trading mechanism is shown in Figure 1.

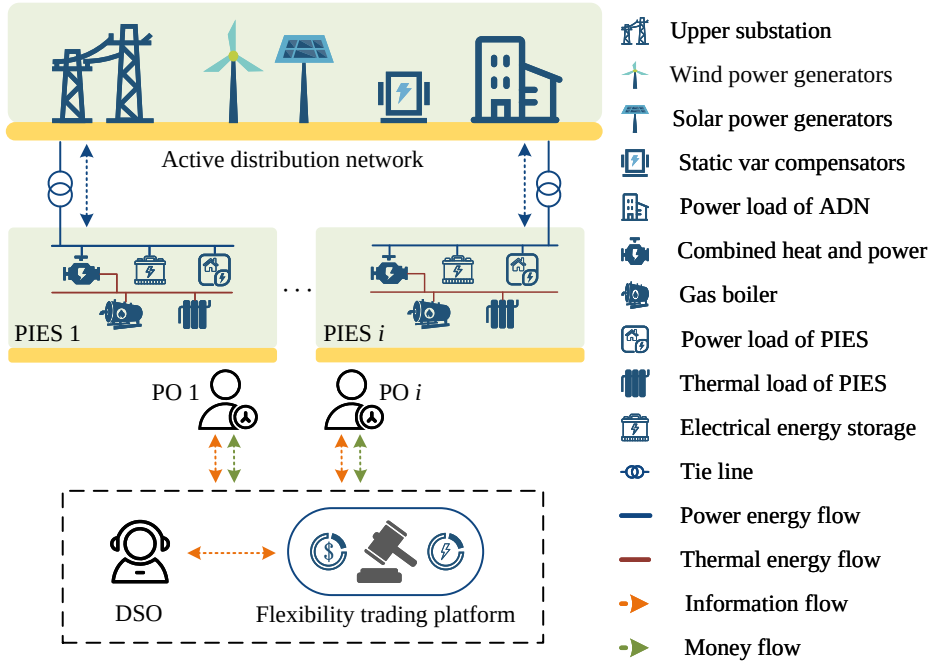

Figure 1. The architecture of the flexibility trading mechanism

2.1 Participated Members

2.1.1 Park-Level Integrated Energy System (PIES)

Each PIES contains power load, thermal load, CHP unit, GB, and ESS. Every PIES can exchange power and gas with ADN and natural gas grid using the tie line and pipeline. By purchasing energy from the external grids and dispatching the internal DERs, the loads of PIES can be satisfied. In addition, two points should be clarified in advance that firstly the dispatching strategies are determined by PO; secondly each PIES provides flexibility for the ADN only after its internal energy balance has been satisfied.

2.1.2 Active Distribution Network (ADN)

ADN refers to a distribution network that possesses the capability to manage energy independently by dispatching inherent solar power generators (SPG), wind power generators (WPG), and static var compensators (SVC). Additionally, DSO is responsible for performing this energy management.

2.1.3 The Operator of PIES (PO)

As the manager of PIES and the supplier of PFR, the main functions of PO include:

1. to develop the optimal day-ahead dispatching plan and submit the power purchasing plan to DSO;
2. to evaluate the capacity of PFR, set its price and send the capacity-price information to DSO in each real-time interval;
3. to determine the optimal real-time dispatching strategy to adjust the day-ahead dispatching plan and provide the reference values for the capacity assessment and pricing models of PFR in next time interval.

2.1.4 The Operator of ADN (DSO)

As the manager of ADN, the demander of PFR and the organizer of the flexibility trading platform, the main responsibilities of DSO are:

1. to develop an optimal transmission power plan from the upper substation based on the power purchasing plans of the multi-PIESs and the forecasted values of RES;
2. to determine the trading amount of PFR by carrying out a real-time economic dispatch involving the actual values of RES and the day-ahead power transmission plan from the substation;
3. to send the trading amount of PFR to each PIES;
4. to utilize a marginal-based method to obtain the market clearing price of PFR.

2.2 Market Transaction Process

The transaction process of the presented flexibility trading mechanism consists of five stages: the planning stage, the declaration stage, the determination stage, the operation stage, and the clearing stage, as depicted in Figure 2. The planning stage happens in the day-ahead period. The other four stages happen in the real-time period.

2.2.1 Planning Stage

The main purpose of the planning stage is to determine the transmission power plan from the substation. To this end, firstly, based on the loads of PIES and

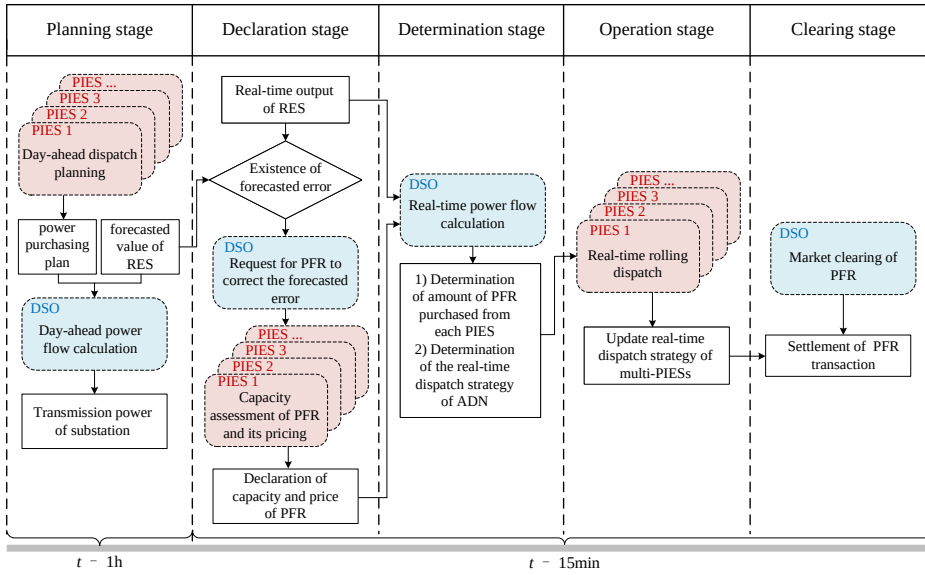

Figure 2. The process of the PFR trading

the installed capacity of DERs, each PO utilizes a day-ahead dispatching model to determine the power purchasing plan. Secondly, based on the power purchasing plans of the multi-PIESs and the day-ahead forecasted values of RES, DSO utilizes a day-ahead dispatching model to calculate the power flow of ADN, of which the transmission power plan from the substation can be determined.

2.2.2 Declaration Stage

In each real-time interval, firstly, DSO determines the forecasted errors of RES according to gaps between the forecasted values and the actual values of RES. And then, DSO requests for the multi-PIESs to provide PFR to help correct the forecasted errors of RES. Afterwards, each PO utilizes a capacity assessment model and a pricing model to determine the capacity and the price of PFR. Finally, each PO declares the capacity-price information of PFR to DSO.

2.2.3 Determination Stage

Based on the capacity-price information of PFR of the multi-PIESs, DSO utilizes a real-time economic dispatching model with involving the network constraints to determine the amount of PFR purchased from each PIES and the real-time dispatching strategy of ADN. And then, DSO sends the trading amount information of PFR to each PO.

2.2.4 Operation Stage

Based on the trading amount of PFR, each PO utilizes a rolling dispatching model to update the dispatching strategy in current time interval and determine the dispatching plan in the future time intervals. Meanwhile, the dispatching strategy in current time interval serves as the reference values for the capacity assessment model and the pricing model of PFR in next time interval.

2.2.5 Clearing Stage

Based on the price of PFR set by each PO and the amount of PFR purchased by DSO, DSO utilizes a marginal-based method to determine the market clearing price of PFR. And then, DSO and the multi-PIESs settle the cost of PFR trading.

3 DAY-AHEAD DISPATCHING MODELS OF PIES AND ADN

3.1 Day-Ahead Dispatching Model of PIES

The structure of an individual PIES is shown in Figure 3. For the simplicity of the modeling, the behavior of the supplying power from PIES to ADN only occurs in the real-time stage and is ignored in the day-ahead stage.

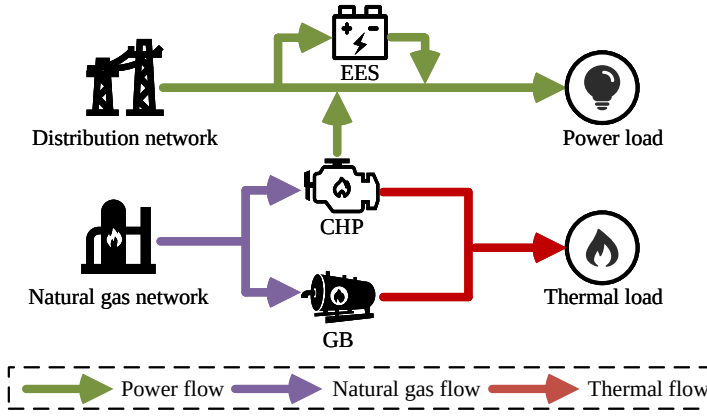

Figure 3. The structure and energy flow of PIES

3.1.1 Objective Function

In the day-ahead stage, PO aims at minimizing the PIES operation cost including the power purchasing cost and the natural gas purchasing cost. Afterwards, PO

sends the power purchasing plan information to DSO. The operation cost is shown in Equation (1).

$$C_{PIES,da}^{k} = \min \sum_{t=1}^{T} \left(\pi_e^t P_{tie}^{k,t} + \pi_g^t G_{gas}^{k,t} \right) \Delta t, \tag{1}$$

where $C_{PIES,da}^{k}$ is the daily operation cost of PIES k; π_e^t and π_g^t are the power price and the natural gas price in the time interval t; $P_{tie}^{k,t}$ is the tie line power of PIES; $G_{gas}^{k,t}$ is the amount of natural gas purchased from the natural gas grid; Δt is the day-ahead time interval; T is the total number of the day-ahead time intervals. Moreover, the value of $P_{tie}^{k,t}$ is always positive, which represents the amount of power purchased from ADN.

3.1.2 Constraints

1. The constraints of the tie line and the pipeline

$$0 \le P_{tie}^{k,t} \le P_{tie}^{\max}, \tag{2}$$

$$0 \le G_{gas}^{k,t} \le G_{gas}^{\max}, \tag{3}$$

   where $P_{tie}^{\max}$ and $G_{gas}^{\max}$ are the maximum transmission power of the tie line and the maximum transmission flow of natural gas pipeline.

2. The constraints of the multi-energy balance

$$P_{tie}^{k,t} + P_{ees,dis}^{k,t} + P_{CHP,e}^{k,t} = P_{ees,ch}^{k,t} + P_{PIES,load,e}^{k,t}, \tag{4}$$

$$P_{GB,h}^{k,t} + P_{CHP,h}^{k,t} = P_{PIES,load,h}^{k,t}, \tag{5}$$

$$G_{gas}^{k,t} = G_{GB,g}^{k,t} + G_{CHP,g}^{k,t}, \tag{6}$$

   where $P_{ees,ch}^{k,t}$ and $P_{ees,dis}^{k,t}$ are the charging and the discharging power of EES in the time interval t; $P_{CHP,e}^{k,t}$ is the power output of CHP in the time interval t; $P_{PIES,load,e}^{k,t}$ indicates the power load of PIES k in the time interval t; $P_{CHP,h}^{k,t}$ is the heat output of CHP in the time interval t; $P_{GB,h}^{k,t}$ is the heat output of the GB in the time interval t; $P_{PIES,load,h}^{k,t}$ indicates the thermal load of PIES k in the time interval t; $G_{GB,g}^{k,t}$ is the gas consumption of the GB in the time interval t; $G_{CHP,g}^{k,t}$ is the gas consumption of CHP in the time interval t.

In addition, the detailed PIES equipment models such as CHP, GB and EES are presented in [25].

3.2 Day-Ahead Dispatching Model of ADN

3.2.1 Objective Function

Based on the power purchasing plans of the multi-PIESs and the day-ahead forecasted values of RES, DSO aims at minimizing the operation cost of ADN, which refers to the cost of the network loss, as shown in Equation (7). As a result, the transmission power plan from the substation can be obtained, which is constant in the real-time stage.

$$C_{ADN,da} = \min \sum_{t=1}^{T} \left[\pi_{loss} \cdot \sum_{ij \in N_{br}} \left(r_{ij} {I_{ij}^t}^2 \right) \right] \Delta t, \tag{7}$$

where $C_{ADN,da}$ is the cost of the daily network loss of ADN; π_{loss} is the unit cost of the network loss; r_{ij} is the branch resistance; I_{ij}^t is the current of branch ij in the time interval t; N_{br} is the set of the branches of ADN.

3.2.2 Constraints

1. The constraints of the AC power flow

$$P_j^t = \sum_{i \in \pi(j)} \left(P_{ij}^t - r_{ij} {I_{ij}^t}^2 \right) - \sum_{m \in \delta(j)} P_{jm}^t, \forall j \in N_B, \tag{8}$$

$$Q_j^t = \sum_{i \in \pi(j)} \left(Q_{ij}^t - x_{ij} {I_{ij}^t}^2 \right) - \sum_{m \in \delta(j)} Q_{jm}^t, \forall j \in N_B, \tag{9}$$

$${V_j^t}^2 = {V_i^t}^2 - 2\left(P_{ij}^t r_{ij} + Q_{ij}^t x_{ij} \right) + {I_{ij}^t}^2 ({r_{ij}}^2 + {x_{ij}}^2), \tag{10}$$

$${I_{ij}^t}^2 = \frac{{P_{ij}^t}^2 + {Q_{ij}^t}^2}{{V_i^t}^2}, \forall ij \in N_{br}, \tag{11}$$

$$P_j^t = P_{ADN,load,j}^t - P_{sub,j}^t + P_{tie,j}^{k,t} - P_{res,j,pre}^t, \tag{12}$$

$$Q_j^t = Q_{ADN,load,j}^t - Q_{sub,j}^t + Q_{SVC,j}^t, \tag{13}$$

where $\pi(j)$ and $\delta(j)$ are the first node set of the branches and the last node set of the branches connected to node j; N_B is the set of the ADN nodes; P_{ij}^t, P_{jm}^t, Q_{ij}^t, and Q_{jm}^t are the active and reactive power flow of the branches; V_i^t and V_j^t are the voltage of node i and node j; P_j^t and Q_j^t are the injected active and reactive power of node j; x_{ij} is the branch reactance; $P_{ADN,load,j}^t$ and $Q_{ADN,load,j}^t$ are the active and reactive power load of node j; $P_{res,j,pre}^t$ is the day-ahead forecasted values of RES, which is connected to node j; $Q_{SVC,j}^t$ indicates the injected reactive power of the SVC, which is connected to node j; $P_{sub,j}^t$ and $Q_{sub,j}^t$ are the active and reactive transmission power from the substation; $P_{tie,j}^t$

represents the tie line power of PIES k in the time interval t, which has been obtained from the day-ahead dispatching model of PIES.

2. The constraints of the power security

$$V_{\min,j}^2 \leq V_j^{t\,2} \leq V_{\max,j}^2, \forall j \in N_B, \tag{14}$$

$$I_{\min,ij}^2 \leq I_{ij}^{t\,2} \leq I_{\max,ij}^2, \forall ij \in N_{br}, \tag{15}$$

where $V_{\min,j}$ and $V_{\max,j}$ are the lower and the upper limits of the node voltage; $I_{\min,ij}$ and $I_{\max,ij}$ are the lower and the upper limits of the branch current.

3. The constraint of SVC

$$Q_{SVC,j}^{\min} \leq Q_{SVC,j}^{t} \leq Q_{SVC,j}^{\max}, \tag{16}$$

where $Q_{SVC,j}^{\min}$ and $Q_{SVC,j}^{\max}$ are the minimum and maximum reactive power outputs of the SVC, which is connected to node j.

4 FLEXIBLE RESOURCE MODELS OF PIES

In the real-time stage, PO can adjust the power output of the internal DERs to change the tie line power between PIES and ADN. This dynamic adjustment ability enables PIES to provide the flexibility for ADN. Therefore, this study regards the change of the tie line power as PFR. The schematic diagram of PFR is shown in Figure 4. In addition, the reference direction of tie line power is from ADN to PIES.

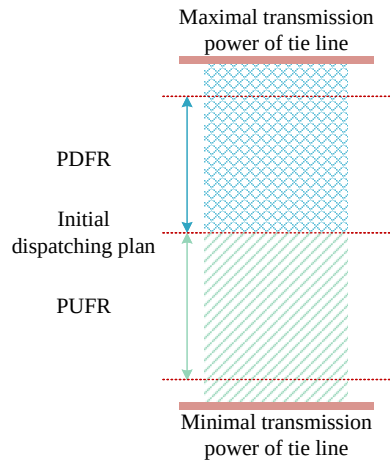

Figure 4. The schematic diagram of PFR

If the output of RES can be predicted accurately, the real-time tie line power of PIES will follow the day-ahead dispatching plan exactly. However, with the

consideration of the RES uncertainty and the dynamic adjustment feature of the tie line power, PO should adjust its transmission power to fulfil the flexibility demand of DSO. This point causes the tie line power to deviate from its initial dispatching plan. Specifically, when the actual value of RES is higher than the forecasted value, PO should increase the tie lie power to accommodate the surplus RES power. This power increment is defined as the PIES downward flexible resource (PDFR). Contrarily, when the actual value of RES is less than the forecasted value, PO should decrease the tie line power and even supply the power for ADN. This power decrement is defined as the PIES upward flexible resource (PUFR). Moreover, it is important to note that PIES can only provide one type of PFR in the real-time interval t'. The mathematical expression of PFR is shown in Equation (17).

$$PFR^{k,t'} = \left\{ -PUFR^{k,t'}, +PDFR^{k,t'} \right\}, \tag{17}$$

where $PFR^{k,t'}$ represents the amount of PFR including $PDFR^{k,t'}$ and $PUFR^{k,t'}$ provided by PIES k in the time interval t'.

4.1 Capacity Assessment Model of PFR

This paper defines the capacity of PFR as the maximum power change of the tie line. Specifically, the capacity of PDFR is the maximum increment of the tie line power, while the capacity of PUFR is the maximum decrement of the tie line power. To determine the capacity of PFR, an optimization-based assessment model is established with an objective to maximize the power change of the tie line, as represented in Equation (18).

$$PFR_{\max}^{k,t'} = \max \Delta P_{tie}^{k,t'}, \tag{18}$$

where $PFR_{\max}^{k,t'}$ is the capacity of PFR including $PDFR_{\max}^{k,t'}$ and $PUFR_{\max}^{k,t'}$; $\Delta P_{tie}^{k,t'}$ is the power change of the tie line. When assessing the capacity of PDFR, $\Delta P_{tie}^{k,t'}$ is always positive. Contrarily, when assessing the capacity of PUFR, $\Delta P_{tie}^{k,t'}$ is always negative.

Besides, the constraints of power energy balance and the tie line power should be satisfied, as shown in Equations (19) and (20).

$$P_{tie}^{k,t'} + \Delta P_{tie}^{k,t'} + P_{ees,dis}^{k,t'} + P_{CHP,e}^{k,t'} = P_{ees,ch}^{k,t'} + P_{PIES,load,e}^{k,t'}, \tag{19}$$

$$P_{tie}^{\min} \le P_{tie}^{k,t'} + \Delta P_{tie}^{k,t'} \le P_{tie}^{\max}, \tag{20}$$

where $P_{tie}^{k,t'}$ is the initial dispatching value of PIES k in the time interval t', which is achieved by solving the rolling dispatching model of PIES (Equations (40), (41), (42), and (43)).

The output characteristics of EES and the ramping limitation of CHP are shown in Equations (21) and (22).

$$E_{ees}^{k,t'} = E_{ees}^{k,t'-\Delta t'}(1-\eta_{loss}^{k}) + \left(P_{ees,ch}^{k,t'}\eta_{ch}^{k} - \frac{P_{ees,dis}^{k,t'}}{\eta_{dis}^{k}}\right)\Delta t', \tag{21}$$

$$-R_{CHP,down}^{k} \le P_{CHP,e}^{k,t'} - P_{CHP,e}^{k,t'-\Delta t'} \le R_{CHP,up}^{k}, \tag{22}$$

where $E_{ees}^{k,t'}$ is the power storage in the time interval t'; η_{loss}^{k}, η_{ch}^{k}, and η_{dis}^{k} are the self-discharge coefficient, the cut-off ratio of the charging, and the discharging process of EES; $\Delta t'$ is the real-time interval; $R_{CHP,down}^{k}$ and $R_{CHP,up}^{k}$ are the lower and the upper limits of the CHP ramping rate in PIES k; $E_{ees}^{k,t'-\Delta t'}$ and $P_{CHP,e}^{k,t'-\Delta t'}$ are also known values, derived from the results of solving the rolling optimization model of PIES (Equations (40), (41), (42), and (43)).

The other constraints are similar to those of the day-ahead dispatching model of PIES (Equations (2), (3), (4), (5), and (6)).

4.2 Pricing Model of PFR

The initial dispatching plan of the tie line power is achieved based on the minimum operation cost of PIES. If PO provides PFR for DSO in the time interval t', the tie line power will deviate from the economical optimal value, resulting in the increase of the operation cost. Therefore, the change of the operation cost before and after the sale of PFR can be utilized as the basis for pricing PFR in the time interval t' using the following steps:

Step 1: The determination of the optimal operation cost after the sale of PFR.

Based on the capacity of PFR in the time interval t', an economic dispatching model of PIES is carried out to obtain the minimum operation cost from the time interval t' to the last time interval. The objective is shown in Equation (23).

$$C_{after\_PFR}^{k,t'-T'} = \min \sum_{t=t'}^{T'} \left(\pi_e^{t'} P_{tie}^{k,t'} + \pi_g^{t'} G_{gas}^{k,t'}\right)\Delta t', \tag{23}$$

where $C_{after\_PFR}^{k,t'-T'}$ is the operation cost from the time interval t' to the last time interval after the sale of the total capacity of PFR in the time interval t'; T' is the total number of the real-time intervals; $P_{tie}^{k,t'}$ represents the tie line power in the time interval t'.

The constraint of power energy balance in the time interval t' needs to consider the case that PO provides the total capacity of PFR, as expressed in Equation (24).

$$P_{tie}^{k,t'} + PFR_{\max}^{k,t'} + P_{ees,dis}^{k,t'} + P_{CHP,e}^{k,t'} = P_{ees,ch}^{k,t'} + P_{PIES,load,e}^{k,t'}. \tag{24}$$

The remaining constraints are similar to those of the day-ahead dispatch model of PIES (Equations (2), (3), (4), (5), and (6)). In addition, it is important that only the tie line power in the time interval t' is the known value, while the tie line power in other time intervals are the decision variables.

Step 2: The calculation of the price of PFR.

Based on the operation cost determined by the model in Step 1, the change of the operation cost before and after the sale of PFR in the time interval t' is achieved. And then, the price of PFR in the time interval t' can be calculated using Equation (25).

$$\pi_{PFR}^{k,t'} = \frac{C_{after\_PFR}^{k,t'-T'} - C_{before\_PFR}^{k,t'-T'}}{PFR_{\max}^{k,t'}}, \tag{25}$$

where $\pi_{PFR}^{k,t'}$ indicates the price of PFR of PIES k in the time interval t', including $\pi_{PUFR}^{k,t'}$ and $\pi_{PDFR}^{k,t'}$; $C_{before\_PFR}^{k,t'-T'}$ represents the minimum operation cost of PIES before the sale of PFR in the time interval t', which is derived from solving the rolling optimization model of PIES in the previous time interval (Equations (40), (41), (42), and (43)).

After determining the capacity and the price of PFR in the time interval t', every PO should send the capacity-price information of PFR to DSO.

5 TRANSACTION MODEL AND MARKET CLEARING METHOD OF PFR

5.1 Real-Time Dispatching Mode of ADN

Based on the capacity-price information of PFR and the actual values of RES, DSO should update the dispatching strategy to avoid serious power curtailment. Therefore, a real-time ADN economic dispatching model with the network constraints is established. Afterwards, the amount of PFR purchased from each PO can be determined, which are further utilized for the market clearing and the rolling optimization of PIES.

5.1.1 Objective Function

The objective is to minimize the real-time comprehensive operation cost of ADN $C_{ADN}^{t'}$ including the network loss $C_{loss}^{t'}$, the renewable power curtailment penalty cost $C_{aban}^{t'}$, the load shedding penalty cost $C_{cut}^{t'}$, and the cost to purchase PFR

$C_{PFR}^{t'}$, as shown in Equations (26), (27), (28), (29), and (30).

$$C_{ADN}^{t'} = \min\left(C_{loss}^{t'} + C_{aban}^{t'} + C_{cut}^{t'} + C_{PFR}^{t'}\right), \tag{26}$$

$$C_{loss}^{t'} = \sum_{ij \in N_{br}} \left(\pi_{loss} r_{ij} I_{ij}^{t'^2}\right) \Delta t', \tag{27}$$

$$C_{aban}^{t'} = \sum_{j \in N_{res}} \pi_{aban} P_{j,aban}^{t'} \Delta t', \tag{28}$$

$$C_{cut}^{t'} = \sum_{j \in N_B} \pi_{cut} P_{j,cut}^{t'} \Delta t', \tag{29}$$

$$C_{PFR}^{t'} = \sum_{k=1}^{N_k} \sum_{j \in N_{PIES}} \pi_{PFR}^{k,t'} PFR_j^{k,t'} \Delta t', \tag{30}$$

where π_{aban} and π_{cut} represent the unit penalty cost of the load shedding and the unit penalty cost of renewable energy curtailment;, N_{res}, N_{PIES}, and N_k indicate the set of nodes of ADN connected to RES, set of nodes of ADN connected to PIES and the number of PIES; $P_{j,aban}^{t'}$ and $P_{j,cut}^{t'}$ are the power of RES curtailment and the load shedding of node j; $PFR_j^{k,t'}$ is the amount of PFR purchased from PIES k, which is connected to node j.

5.1.2 Real-Time Constraints

1. The constraint of load shedding

$$0 \leq P_{j,cut}^{t'} \leq P_{ADN,load,j}^{t'}. \tag{31}$$

   Equation (31) indicates the constraint of load shedding of node j; $P_{ADN,load,j}^{t'}$ represents the power load of node j in the time interval t'.

2. The constraint of RES curtailment

$$0 \leq P_{j,aban}^{t'} \leq P_{res,j,real}^{t'}. \tag{32}$$

   Equation (32) represents the constraint of the RES curtailment of node j; $P_{res,j,real}^{t'}$ is the actual output of RES connected to node j in the time interval t'.

3. The constraint of node power balance

$$P_j^{t'} = (P_{ADN,load,j}^{t'} - P_{j,loss}^{t'}) - (P_{res,j,real}^{t'} - P_{j,aban}^{t'}) - P_{sub,j}^{t'} + P_{tie,j}^{k,t'} + PFR_j^{k,t'}. \tag{33}$$

   Equation (33) shows the constraint of node power balance; $P_j^{t'}$ is the injected active power of node j; $P_{sub,j}^{t'}$ represents the transmission power from the upper

grid, which is determined by solving the day-ahead dispatching model of ADN; $P_{tie,j}^{k,t'}$ is the initial tie line power of PIES k connected to node j, which equals $P_{tie}^{k,t'}$.

4. The constraints of PFR

$$PFR_j^{k,t'} = PUFR_j^{k,t'} + PDFR_j^{k,t'}, \tag{34}$$

$$0 \leq PUFR_j^{k,t'} \leq PUFR_{\max}^{k,t'} \cdot u^{k,t'}, \tag{35}$$

$$0 \leq PDFR_j^{k,t'} \leq PDFR_{\max}^{k,t'} \cdot (1 - u^{k,t'}). \tag{36}$$

Equations (34), (35), and (36) are the constraints of PFR of PIES k connected to node j; $u^{k,t'}$ is set to 0 or 1; 0 means PIES k sells PDFR in the time interval t', while 1 means PIES k sells PUFR in the time interval t'.

5. The constraints of flexibility demand

The forecasted errors of RES are taken as the flexibility demand of DSO, as shown in Equation (37) and (38). Besides, the detailed models of forecasted errors of RES such as SPG and WPG can be found in [26].

$$D_{PUFR}^{t'} = \left| P_{res,j,real}^{t'} - P_{res,j,pre}^{t'} \right|, \quad P_{res,j,real}^{t'} < P_{res,j,pre}^{t'}, \tag{37}$$

$$D_{PDFR}^{t'} = \left| P_{res,j,real}^{t'} - P_{res,j,pre}^{t'} \right|, \quad P_{res,j,real}^{t'} > P_{res,j,pre}^{t'}, \tag{38}$$

where $D_{PUFR}^{t'}$ and $D_{PDFR}^{t'}$ represent the upward flexibility demand and the downward flexibility demand in the time interval t'.

The other constraints have been presented in the day-ahead dispatching model (Equations (8), (9), (10), (11), (12), (13), (14), (15), and (16)).

5.2 Marginal-Based Clearing Method

To clear the PFR market in each real-time interval, this paper presents a marginal-based method [27], which not only enables each PO to earn marginal profit, but also reduces the cost for DSO to handle the uncertainty of RES, thus achieving the maximum social welfare. Based on the trading amount of PFR and its price set by each PO, the schematic of the market clearing is shown in Figure 5.

As can be seen from Figure 5, the market clearing price of PFR is the highest price of PFR set by PO k. Therefore, if the offered price of PFR is less than the market clearing price, PO can have marginal revenue, as shown in the shaded part of Figure 5. And the marginal revenue of PIES k is determined by Equation (39).

$$F_{PFR}^{k,t'} = (\pi_{cl}^{t'} - \pi_{PFR}^{k,t'}) \cdot PFR^{k,t'}, \tag{39}$$

where $F_{PFR}^{k,t'}$ indicates the marginal revenue of PIES k in the time interval t' after the sale of PFR; $\pi_{cl}^{t'}$ represents the market clearing price of PFR in the time interval t'.

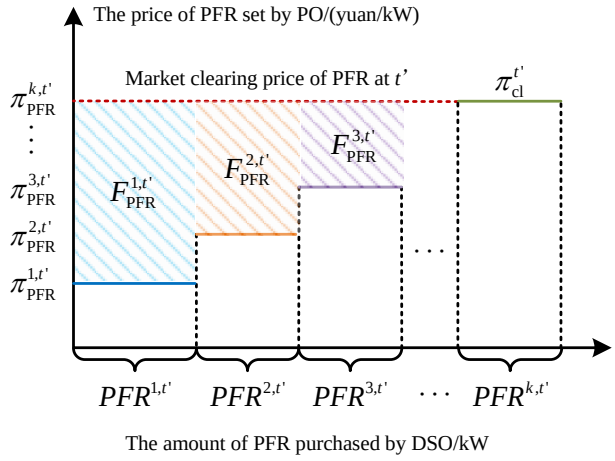

Figure 5. The schematic of market clearing of PFR in the time interval t'

6 REAL-TIME ROLLING DISPATCHING MODEL OF PIES

During the real-time stage, the tie line power of PIES no longer follows the day-ahead plan. Instead, it varies with the flexibility demand of DSO, which causes a deviation from the dispatching plan and might increase the operation cost. Therefore, to realize the economic operation of PIES, PO should update the dispatching strategy based on the real-time trading amount of PFR and the real-time DER operational status. Therefore, a rolling optimization method is employed to implement the dispatching strategy of PIES.

6.1 Objective Function

PO aims at minimizing the operation cost including the cost of purchasing power and the cost of purchasing natural gas from the time interval t' to the last time interval, as shown in Equation (40).

$$C_{PIES}^{k,t'-T'} = \min \sum_{t=t'}^{T'} \left(\pi_e^{t'} P_{tie}^{k,t'} + \pi_g^{t'} G_{gas}^{k,t'} \right) \Delta t', \tag{40}$$

where $C_{PIES}^{k,t'-T'}$ indicates the operation cost of PIES k from the time interval t' to the last time interval. Different from Equation (4), Equation (41) takes the trading amount of PFR into account and the time interval is smaller.

6.2 Real-Time Constraints

6.2.1 The Constraint of Power Balance

$$P_{tie}^{k,t'} + PFR^{k,t'} + P_{ees,dis}^{k,t'} + P_{CHP,e}^{k,t'} = P_{ees,ch}^{k,t'} + P_{PIES,load,e}^{k,t'}. \tag{41}$$

Equation (41) shows the constraint of the power balance with involving the trading amount of PFR; $PFR^{k,t'}$ is the amount of PFR purchased by DSO in the time interval t', which equals $PFR_j^{k,t'}$.

6.2.2 The Constraint of Ramping Capacity

$$-R_{CHP,down}^{k} \leq P_{CHP,e}^{k,t'} - P_{CHP,e}^{k,t'-\Delta t'} \leq R_{CHP,up}^{k}. \tag{42}$$

Equation (42) indicates the constraint of the ramping capacity of CHP units; $P_{CHP,e}^{k,t'}$ is the power output of CHP in the time interval t', which is a decision variable; $P_{CHP,e}^{k,t'-\Delta t'}$ is the power output of CHP in the previous time interval $t' - \Delta t'$, which is a known value by solving the rolling dispatching model in the previous optimization period (from $t' - \Delta t'$ to T').

6.2.3 The Constraints of Energy Storage

$$E_{ees}^{k,t'} = E_{ees}^{k,t'-\Delta t'} \left(1 - \eta_{loss}^{k}\right) + \left(P_{ees,ch}^{k,t'} \eta_{ch}^{k} - \frac{P_{ees,dis}^{k,t'}}{\eta_{dis}^{k}}\right) \Delta t'. \tag{43}$$

Equation (43) shows the constraint of the energy storage, where $E_{ees}^{k,t'-\Delta t'}$ is also a known value. The other constraints are the same as those of the day-ahead dispatch model (Equations (2), (3), (4), (5), and (6)).

The decision variables of this model are the power output of DERs and the energy purchasing plan from the time interval t' to the last time interval. After solving this model, only the dispatch strategy in the time interval t' will be accepted by PO. In addition, the tie line power $P_{tie}^{k,t'+\Delta t'}$ in the time interval $(t' + \Delta t')$ and the operation cost $C_{base}^{k,(t'+\Delta t)-T'}$ will be utilized as the reference values for the capacity assessment model and the pricing model of PFR in next time interval $(t' + \Delta t')$.

7 MODEL PROCESSING AND SOLUTION

7.1 Second-Order Cone Relaxation on the Power Flow Model

Due to the nonlinear terms contained in the AC power flow constraints, it is difficult to directly solve the day-ahead and the real-time dispatching model of ADN. Therefore, the second-order cone relaxation method is adopted to transform the power flow constraints into the second-order cone constraints [26]. Firstly, take ${I_{ij}^{t}}^2 = \tilde{I}_{ij}^{t}$, $V_i^{t2} = \tilde{V}_i^{t}$, and substitute them into Equations (8), (9), (10), and (11). Afterwards,

perform the second-order relaxation on Equation (11). Consequently, Equations (8), (9), (10), and (11) can be transformed to:

$$P_j^t = \sum_{i\in\pi(j)} \left(P_{ij}^t - r_{ij}\tilde{I}_{ij}^t\right) - \sum_{m\in\delta(j)} P_{jm}^t, \quad \forall j \in N_B, \tag{44}$$

$$Q_j^t = \sum_{i\in\pi(j)} \left(Q_{ij}^t - x_{ij}\tilde{I}_{ij}^t\right) - \sum_{m\in\delta(j)} Q_{jm}^t, \quad \forall j \in N_B, \tag{45}$$

$$\tilde{V}_j^t = \tilde{V}_i^t - 2\left(P_{ij}^t r_{ij} + Q_{ij}^t x_{ij}\right) + \tilde{I}_{ij}^t\left({r_{ij}}^2 + {x_{ij}}^2\right), \tag{46}$$

$$\left\| \begin{array}{c} 2P_{ij}^t \\ 2Q_{ij}^t \\ \tilde{I}_{ij}^t - \tilde{V}_i^t \end{array} \right\|_2 \leq \tilde{I}_{ij}^t + \tilde{V}_i^t, \quad \forall ij \in N_{br}. \tag{47}$$

As a result, the nonlinear power flow constraints have been processed into second-order cone constraints.

7.2 Rolling Optimization Based on Model Predictive Control (MPC)

To ensure the energy balance constraints of PIES after the sale of PFR, a rolling optimization method based on MPC is adopted to determine the accurate dispatching strategy of PIES [28]. The optimization scheme is shown in Figure 6. In terms of providing a better explanation, taking the time interval $t_0^{'} + \Delta t'$ as an example:

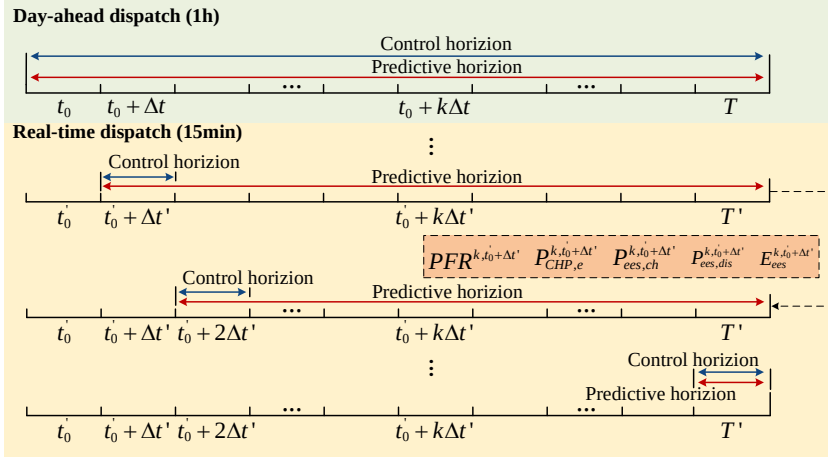

Figure 6. The schematic illustration of the rolling optimization method based on MPC

Step 1: The optimization of the dispatching strategies in the current predictive horizon.

Firstly, based on the forecasted values of the loads in the predictive horizon (from the time interval $t_0^{'} + \Delta t'$ to the last time interval), the trading amount of PFR in the time interval $t_0^{'} + \Delta t'$ and the running status of CHP and EES in the previous time interval $t_0^{'}$, PO aims at minimizing the operation cost from the time interval $t_0^{'} + \Delta t'$ to the last time interval. And then, the dispatching plan of PIES in the predictive horizon can be obtained, of which only the dispatching plan in the time interval $t_0^{'} + \Delta t'$ will be carried out.

Step 2: The optimization of the dispatching strategies in the next predictive horizon.

Afterwards, in next optimization period, the predictive horizon is updated from the time interval $t_0^{'} + 2\Delta t'$ to the last time interval. Therefore, based on the running status of CHP and EES in the previous time interval $t_0^{'} + \Delta t'$ and the trading amount of PFR in the time interval $t_0^{'} + 2\Delta t'$, PO optimizes the operation cost of PIES from the time interval $t_0^{'} + 2\Delta t'$ to the last time interval. Similarly, only the dispatching strategy in the time interval $t_0^{'} + 2\Delta t'$ will be carried out.

Finally, the optimization period is constantly updated until the dispatching strategy in all time interval is obtained.

7.3 Model Solution

The models presented in this paper, including the capacity assessment model of PFR, the pricing model of PFR, the day-ahead dispatching models of PIES and ADN, and the real-time dispatching models of PIES and ADN, belong to the mixed integer linear programming problems (MILP). For the sake of clear presentation, the above models are rewritten in the compact form, as shown in Equation (48).

$$\begin{cases} \min & f(x,u), \\ \text{s.t.} & g(x,u) \leq 0, \\ & h(x,u) = 0, \end{cases} \tag{48}$$

where x are the continuous variables; u are the integer variables; $g(*)$ and $h(*)$ indicate the inequality constraints and the equality constraints. To solve the above problems, this paper employs the commercial solver GUROBI [25].

8 CASE STUDY

8.1 Case Parameters

In this paper, a modified 33-bus ADN system with SPG, WPG and the multi-PIESs with three PIESs three PIESs is selected for the case study and all the parameters are

taken from [26, 29]. The structure of the system is shown in Figure 7. Specifically, three PIESs are connected to ADN at nodes 7, 8, and 9. WPG and SPG are connected to ADN at nodes 6 and 10. To satisfy the voltage constraints, two SVC devices are connected to ADN at nodes 18 and 33, of which the adjustment capability is −0.1 1 Mvar. The parameters of CHP, ESS, GB, tie line, and pipeline are listed in Table 1. The time-of-use power price, the unit cost of network loss, the unit penalty cost of RES curtailment, and the unit penalty cost of load shedding are shown in Table 2. The price of gas is 3.24 yuan/m3. The day-ahead and intra-day forecasted data of WPG and SPG are shown in Figures 8 c) and 8 b). Due to the high accuracy of short-term load forecasting, the forecasted errors of power loads in three PIESs and ADN are ignored. The power loads of each PIES and ADN are shown in Figure 8 d). The thermal loads of each PIES are shown in Figure 8 e). Besides, it is assumed that the day-ahead dispatching includes 24 periods with the time interval of 1 hour. The real-time dispatching includes 96 periods with the time interval of 15 minutes.

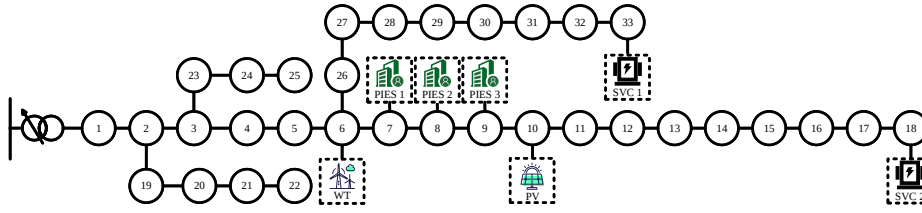

Figure 7. The structure of the modified IEEE 33 distribution system

		PIES 1	PIES 2	PIES 3
CHP	Rated capacity/kW	800	600	900
	Upward ramp/(kW/h)	400	300	450
	Downward ramp/(kW/h)	400	300	450
	Power production efficiency	0.35	0.35	0.35
	Heat production efficiency	0.29	0.29	0.29
GB	Rated capacity/kW	500	400	400
	Heat production efficiency	0.87	0.87	0.87
EES	Maximal capacity/kW	500	500	500
	Minimal capacity/kW	100	100	100
	Maximal discharge power/(kW/h)	350	350	350
	Charging efficiency	0.9	0.9	0.9
	Discharging efficiency	0.95	0.95	0.95
	Self-loss rate	0.05	0.05	0.05

Table 1. Distributed energy resources parameters

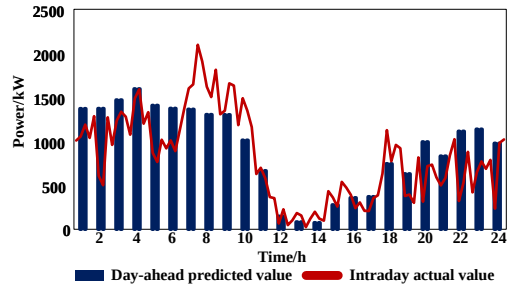

a) WPG output

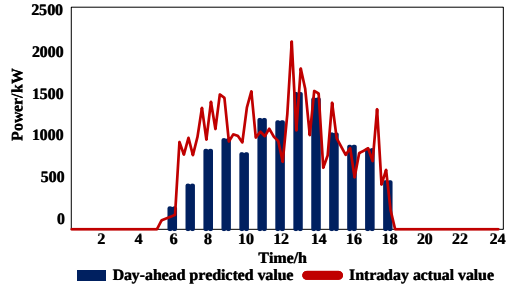

b) SPG output

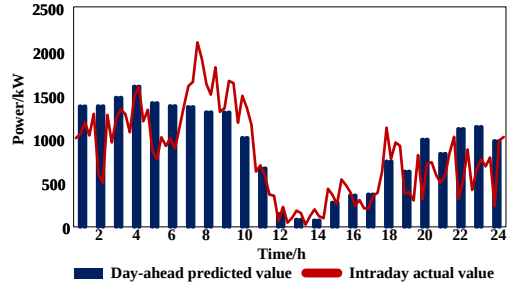

c) WPG output

	Period	Price/(yuan/kWh)
Peak period	7:00–11:00 19:00–23:00	1.26
Flat period	11:00–19:00	0.84
Valley period	1:00–7:00 23:00–1:00	0.43
The unit cost of network loss	1:00–24:00	1.00
The unit penalty cost of RES curtailment	1:00–24:00	0.96
The unit penalty cost of load shedding	1:00–24:00	0.85

Table 2. Relative prices parameters

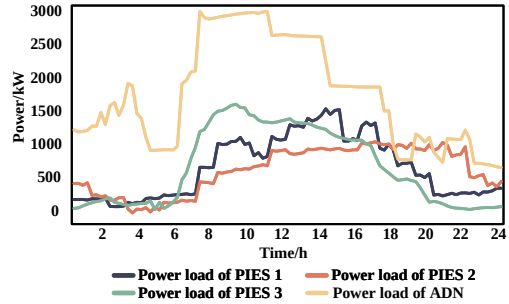

d) Power load of each PIES and ADN

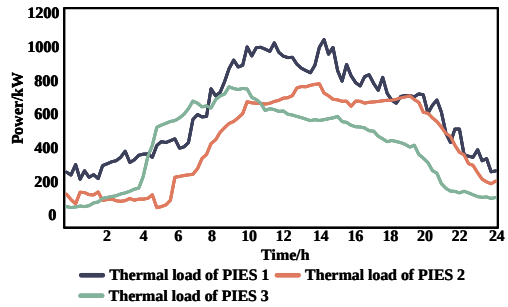

e) Thermal load of each PIES

Figure 8. Power load, Thermal load and RES output

8.2 Analysis of Operational Flexibility of ADN

Figures 9 and 10 illustrate the balance between the upward/downward flexibility demand of ADN and PUFR/PDFR supplied by each PIES. The results demonstrate that PFR fully meets the flexibility demand of ADN during most dispatching intervals. When the flexibility demand is low, a single PIES can supply sufficient PFR. During high flexibility demand intervals, all three PIESs need to contribute PFR. However, load shedding and RES curtailment still occur in certain time intervals. The reasons can be summarized as follows: firstly, the high forecasted errors of RES results in the increase of the flexibility demand during these time intervals; secondly, the capacities of PFR of three PIESs are not adequate to meet the high flexibility demand. Therefore, DSO has to implement power curtailment to ensure the power balance.

Overall, with the provision of PFR, DSO can utilize the local FR to mitigate the uncertainty of WPG and SPG. As a result, the real-time power balance can be guaranteed without any adverse impacts on the transmission power of the substation.

The variation of the node voltage is shown in Figure 11. It can be observed that the voltage level of each node remains within the permitted operational limits.

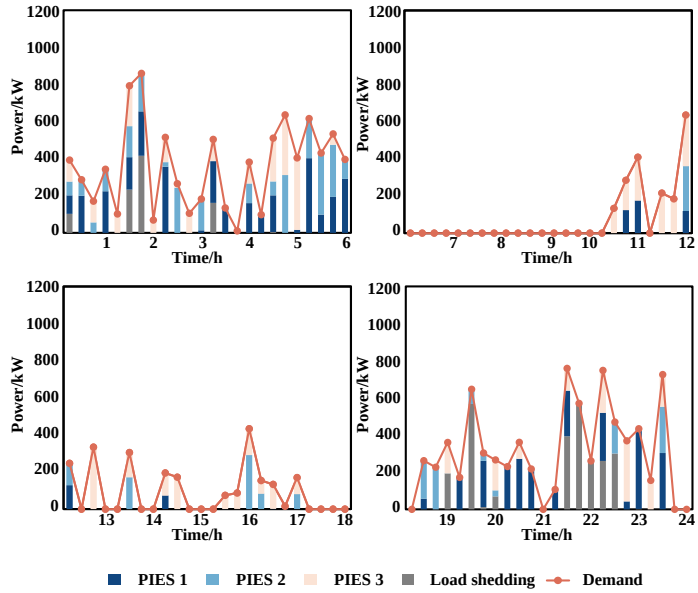

Figure 9. Share of each PIES in supplying PUFR

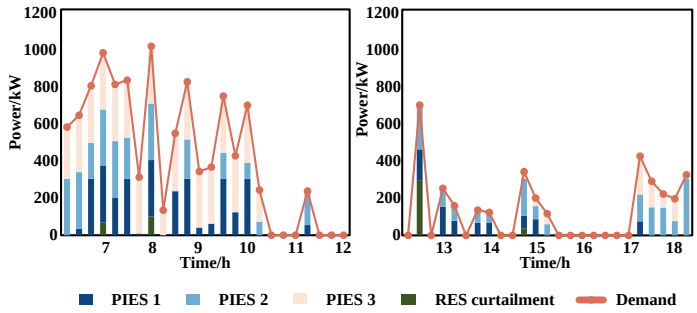

Figure 10. Share of each PIES in supplying PDFR

Compared to the traditional trading mechanism, the transaction model presented in this paper involves the power flow constraints so that it firstly helps avoid violating the voltage constraint and guaranteeing the operation security of ADN. Secondly, it is able to ensure the feasibility of the trading results.

Figures 12 a) and 12 b) show the results of the load shedding and the RES curtailment before and after the sale of PFR. With involving PFR, the amount of the load shedding and the RES curtailment have been significantly reduced. In most time intervals, the load shedding power and the RES curtailment power seldom occur. This point indicates that ADN has affluent operational flexibility using the

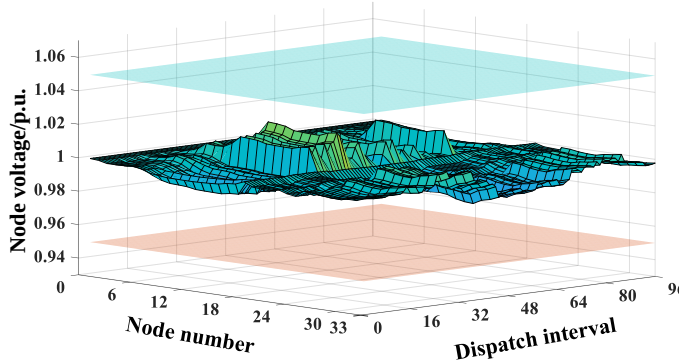

Figure 11. The variation of node voltage in ADN

PFR supplied by three PIESs. Statistically, the load shedding power decreases by 82.60 %. The RES curtailment power decreases by 96.45 %.

8.3 Analysis of Dispatching Strategies of Multi-PIESs

Taking PIES 1 as an example, Figure 13 illustrates a comparison of the tie line power before and after the sale of PFR. The tie line power of PIES 1 is positive before the sale of PFR due to the constraint that the power supply from PIES to ADN is only permitted after the sale of PFR. Before the sale of PFR, PO aims at minimizing the operation cost of PIES based on the time-of-use power price. Specifically, during the valley and flat price periods, the power price is relatively low. Therefore, PO increases the tie line power to purchase more power from ADN to meet the internal power load demand. During the peak price period, the power price is high, which causes a sharp decrease in the tie line power.

After the sale of PFR, it can be seen that the tie line power of PIES 1 is either positive or negative. The reason is that PIES 1 sells PFR to DSO, which causes the tie line power no longer strictly follows the dispatching plan. Instead, the tie line power varies with the flexibility demand of DSO. Specifically, when the actual values of WPG and SPG exceeds the forecasted values (from 1:00 to 6:00), PO increases the tie line power to provide PDFR. Contrarily (from 7:00 to 10:00), PO decreases the tie line power or even reverses the direction of the tie line power to sell PUFR.

It indicates that the presented flexibility trading mechanism enables the bi-directional interactions among three PIESs and ADN to handle the uncertainty of RES from two aspects: firstly, PIES can act as a flexible load to accommodate the surplus RES power; secondly, PIES can act as a flexible power source to supply power to ADN for the power loss of RES.

To analyze the contribution of CHP in the provision of PFR, Figure 14 shows the change of its power output before and after the sale of PFR. Before the sale of

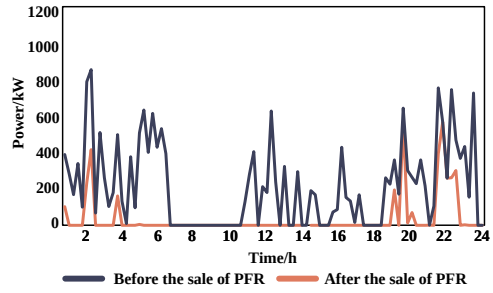

a) Comparison of load shedding before and after the sale of PFR

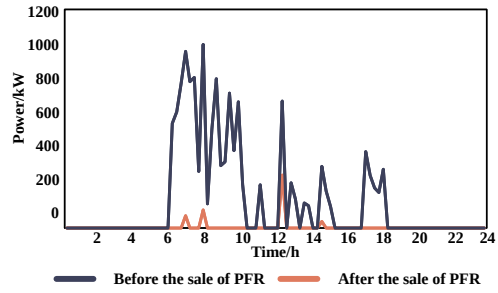

b) Comparison of RES curtailment before and after the sale of PFR

Figure 12. Comparison of power curtailment before and after the sale of PFR

PFR, PO manages the output of CHP to minimize the operation cost of PIES based on the time-of-use power price. After the sale of PFR, the power output of CHP is affected by the trading amount of PFR. When the actual value of RES is lower than the forecasted value (1:00–6:00 and 11:00–13:00), PO increases the power output of CHP to raise the tie line power to sell PUFR. When the actual value of RES is larger than the forecasted value (7:00–10:00, 15:00, and 18:00), PO decreases the power output of CHP to lower the tie line power to sell PDFR.

8.4 Analysis of Operation Cost

Table 3 represents the comparison of the operation cost of DSO in different stages. Before the sale of PFR, DSO can only implement the load shedding and the RES curtailment to maintain the power balance. However, the penalty price of the power curtailment is high, which results in a significant increase of the operation cost. After the sale of PFR, DSO can purchase PFR to handle the uncertainty of RES. Since the price of PFR is much lower than the unit penalty cost, the operation cost of DSO decreases by 30.70 %.

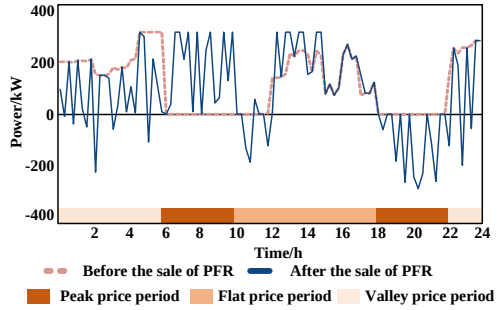

Figure 13. The comparison of tie line power of PIES 1 before and after the sale of PFR

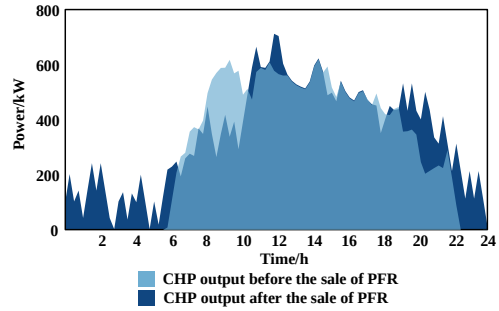

Figure 14. The comparison of the power output of CHP in PIES 1 before and after the sale of PFR

Table 4 presents the operation cost of three PIESs before and after the sale of PFR. Due to the update of the dispatching strategy of PIES, both the costs of purchasing power and natural gas increase after the sale of PFR. However, despite the increase in the energy purchasing cost, PO earns a considerable profit by selling PFR. As a result, the net operation cost of each PIES is reduced to: 7.1 % for PIES 1, 4.9 % for PIES 2, and 12.44 % for PIES 3.

	Day-Ahead Stage	Real-Time Stage	
		Before the sale of PFR	After the sale of PFR
Cost for network loss [yuan]	355.96	295.77	347.26
Cost for RES curtailment [yuan]	0	2 959.95	104.97
Cost for load shedding [yuan]	0	4 988.99	868.20
Cost for the PFR [yuan]	0	0	3 487.52
Total operation cost [yuan]	355.96	8 244.71	4 807.96
Cost reduction [yuan]	–	–	3 436.75

Table 3. The comparison of operation cost of DSO in different scenarios

	Before the sale of PFR			After the sale of PFR		
	PIES 1	PIES 2	PIES 3	PIES 1	PIES 2	PIES 3
Cost for buying electricity [yuan]	1 540.5	1 568.7	2 316.1	2 192.6	2 307.9	3 153.8
Cost for buying gas [yuan]	7 612.9	6 715.5	6 634.3	8 229.3	6 931.0	6 804.9
Profit by selling PFR [yuan]	–	–	–	1 914.8	1 363.3	2 122.0
Total net cost [yuan]	9 153.4	8 284.2	8 950.4	8 507.1	7 875.6	7 836.7
Cost reduction [yuan]	–		–	646.3	408.6	1 113.7

Table 4. The comparison of operation cost of three PIESs

9 CONCLUSION

To realize the marketization of FR and improve the operational flexibility of ADN, this paper presents a local flexibility trading mechanism to motivate the multi-PIESs to trade PFR with DSO. Firstly, by tapping the dynamic adjustment feature contained in the tie line power, an optimization-based method is employed to evaluate the capacity of PFR. Secondly, based on the cost change of PIES before and after the sale of PFR, a pricing model of PFR is established. And then, an ADN economic dispatch model with involving the network constraints is set up to determine the trading amount of PFR. Afterwards, a rolling optimization method based on MPC is applied to obtain the accurate dispatching strategy of PIES. Finally, all models are transformed into MILP problems and solved using the GUROBI solver. In general, experimental results demonstrate the following points:

1. The flexibility trading mechanism presented in this paper can effectively improve the system operational flexibility. Consequently, with the provision of PFR, the power of the load shedding and the RES curtailment have decreased by 82.60 % and 96.45 %, respectively.
2. After the sale of PFR, the operation economy of each market participated member has been significantly improved. Specifically, the comprehensive operation cost of ADN has decreased by 41.68 %. Meanwhile, the net operation cost of each PIES has decreased to different degrees: 7.1 % for PIES 1, 4.9 % for PIES 2, and 12.44 % for PIES 3.
3. In terms of the operation security of ADN, the presented economic dispatch model involves the network constraints, which guarantees the security and stability of ADN.

For future work, the game behaviors among DSO and other market players such as virtual power plants and electric vehicles can be further investigated to design a more adaptive flexibility trading mechanism.

REFERENCES

[1] El Amine, A.—Hassan, H. A. H.—Nuaymi, L.: Battery-Aware Green Cellular Networks Fed by Smart Grid and Renewable Energy. IEEE Transactions on Network and Service Management, Vol. 18, 2021, No. 2, pp. 2181–2192, doi: 10.1109/TNSM.2020.3038302.

[2] Pamshetti, V. B.—Singh, S.—Thakur, A. K.—Singh, S. P.—Babu, T. S.—Patnaik, N.—Krishna, G. H.: Cooperative Operational Planning Model for Distributed Energy Resources with Soft Open Point in Active Distribution Network. IEEE Transactions on Industry Applications, Vol. 59, 2023, No. 2, pp. 2140–2151, doi: 10.1109/TIA.2022.3223339.

[3] Russo, M. A.—Carvalho, D.—Martins, N.—Monteiro, A.: Forecasting the Inevitable: A Review on the Impacts of Climate Change on Renewable Energy Resources. Sustainable Energy Technologies and Assessments, Vol. 52, 2022, Art. No. 102283, doi: 10.1016/j.seta.2022.102283.

[4] Li, Y.—Yang, Z.—Li, G.—Zhao, D.—Tian, W.: Optimal Scheduling of an Isolated Microgrid with Battery Storage Considering Load and Renewable Generation Uncertainties. IEEE Transactions on Industrial Electronics, Vol. 66, 2019, No. 2, pp. 1565–1575, doi: 10.1109/TIE.2018.2840498.

[5] Hu, Y. X.—Wang, M. Q.—Yang, M.—Wang, M. X.—Zhao, L. M.—Ding, T. C.—Xu, D. P.: Economic Dispatch of Active Distribution Network Considering Admissible Region of Net Load Based on New Injection Shift Factors. International Journal of Electrical Power & Energy Systems, Vol. 145, 2023, Art. No. 108641, doi: 10.1016/j.ijepes.2022.108641.

[6] Rayati, M.—Bozorg, M.—Cherkaoui, R.—Carpita, M.: Distributionally Robust Chance Constrained Optimization for Providing Flexibility in an Active Distribution Network. IEEE Transactions on Smart Grid, Vol. 13, 2022, No. 4, pp. 2920–2934, doi: 10.1109/TSG.2022.3154023.

[7] Alhelou, H. H.—Heydarian-Forushani, E.—Siano, P.: Flexibility in Electric Power Distribution Networks. CRC Press, 2021.

[8] Ghaemi, S.—Salehi, J.—Moeini-Aghtaie, M.: Developing a Market-Oriented Approach for Supplying Flexibility Ramping Products in a Multimicrogrid Distribution System. IEEE Transactions on Industrial Informatics, Vol. 17, 2021, No. 10, pp. 6765–6775, doi: 10.1109/TII.2020.3047600.

[9] Zhang, D.—Hu, Y.—Gao, Y.: Flexibility Improvement of CHP Unit for Wind Power Accommodation. Journal of Modern Power Systems and Clean Energy, Vol. 10, 2022, No. 3, pp. 731–742, doi: 10.35833/MPCE.2020.000630.

[10] Beiron, J.—Göransson, L.—Normann, F.—Johnsson, F.: Flexibility Provision by Combined Heat and Power Plants – An Evaluation of Benefits from a Plant and System Perspective. Energy Conversion and Management: X, Vol. 16, 2022, Art. No. 100318, doi: 10.1016/j.ecmx.2022.100318.

[11] Alipour, M.—Gharehpetian, G. B.—Ahmadiahangar, R.—Rosin, A.—Kilter, J.: Energy Storage Facilities Impact on Flexibility of Active Distribution Networks: Stochastic Approach. Electric Power Systems Research, Vol. 213, 2022, Art. No. 108645, doi: 10.1016/j.epsr.2022.108645.

[12] Zhang, Y.—Wang, X.—He, J.—Xu, Y.—Pei, W.: Optimization of Distributed Integrated Multi-Energy System Considering Industrial Process Based on Energy Hub. Journal of Modern Power Systems and Clean Energy, Vol. 8, 2020, No. 5, pp. 863–873, doi: 10.35833/MPCE.2020.000260.

[13] Sperstad, I. B.—Degefa, M. Z.—Kjølle, G.: The Impact of Flexible Resources in Distribution Systems on the Security of Electricity Supply: A Literature Review. Electric Power Systems Research, Vol. 188, 2020, Art. No. 106532, doi: 10.1016/j.epsr.2020.106532.

[14] Li, Z.—Xu, Y.: Optimal Coordinated Energy Dispatch of a Multi-Energy Microgrid in Grid-Connected and Islanded Modes. Applied Energy, Vol. 210, 2018, pp. 974–986, doi: 10.1016/j.apenergy.2017.08.197.

[15] Cheng, L.—Wan, Y.—Qi, N.—Zhou, Y.: Coordinated Operation Strategy of Distribution Network with the Multi-Station Integrated System Considering the Risk of Controllable Resources. International Journal of Electrical Power & Energy Systems, Vol. 137, 2022, 107793 pp., doi: 10.1016/j.ijepes.2021.107793.

[16] Liu, Y.—Guo, L.—Wang, C.: A Robust Operation-Based Scheduling Optimization for Smart Distribution Networks with Multi-Microgrids. Applied Energy, Vol. 228, 2018, pp. 130–140, doi: 10.1016/j.apenergy.2018.04.087.

[17] Ostovar, S.—Moeini-Aghtaie, M.—Hadi, M. B.: Designing a New Procedure for Participation of Prosumers in Day-Ahead Local Flexibility Market. International Journal of Electrical Power & Energy Systems, Vol. 146, 2023, Art. No. 108694, doi: 10.1016/j.ijepes.2022.108694.

[18] Jin, X.—Wu, Q.—Jia, H.: Local Flexibility Markets: Literature Review on Concepts, Models and Clearing Methods. Applied Energy, Vol. 261, 2020, Art. No. 114387, doi: 10.1016/j.apenergy.2019.114387.

[19] Olivella-Rosell, P.—Bullich-Massagué, E.—Aragüés-Peñalba, M.—Sumper, A.—Ottesen, S. Ø.—Vidal-Clos, J. A.—Villafáfila-Robles, R.: Optimization Problem for Meeting Distribution System Operator Requests in Local Flexibility Markets with Distributed Energy Resources. Applied Energy, Vol. 210, 2018, pp. 881–895, doi: 10.1016/j.apenergy.2017.08.136.

[20] Torbaghan, S. S.—Blaauwbroek, N.—Kuiken, D.—Gibescu, M.—Hajighasemi, M.—Nguyen, P.—Smit, G. J. M.—Roggenkamp, M.—Hurink, J.: A Market-Based Framework for Demand Side Flexibility Scheduling and Dispatching. Sustainable Energy, Grids and Networks, Vol. 14, 2018, pp. 47–61, doi: 10.1016/j.segan.2018.03.003.

[21] Jia, Y.—Wan, C.—Yu, P.—Song, Y.—Ju, P.: Security Constrained P2P Energy Trading in Distribution Network: An Integrated Transaction and Operation Model. IEEE Transactions on Smart Grid, Vol. 13, 2022, No. 6, pp. 4773–4786, doi: 10.1109/TSG.2022.3159322.

[22] Li, J.—Zhang, C.—Xu, Z.—Wang, J.—Zhao, J.—Zhang, Y. J. A.: Distributed Transactive Energy Trading Framework in Distribution Networks. IEEE Transactions on Power Systems, Vol. 33, 2018, No. 6, pp. 7215–7227, doi: 10.1109/TPWRS.2018.2854649.

[23] Lin, X.—Wang, L.—Xu, H.—Yang, M.—Cheng, X.: Event-Trigger Rolling

Horizon Optimization for Congestion Management Considering Peer-to-Peer Energy Trading Among Microgrids. International Journal of Electrical Power & Energy Systems, Vol. 147, 2023, Art. No. 108838, doi: 10.1016/j.ijepes.2022.108838.

[24] Cao, Z.—Han, Y.—Wang, J.—Zhao, Q.: Two-Stage Energy Generation Schedule Market Rolling Optimisation of Highly Wind Power Penetrated Microgrids. International Journal of Electrical Power & Energy Systems, Vol. 112, 2019, pp. 12–27, doi: 10.1016/j.ijepes.2019.04.037.

[25] Liu, Y.—Chen, X.—Wu, L.—Ye, Y.: Distributionally Robust Economic Dispatch Using IDM for Integrated Electricity-Heat-Gas Microgrid Considering Wind Power. CSEE Journal of Power and Energy Systems, Vol. 9, 2023, No. 3, pp. 1182–1192, doi: 10.17775/CSEEJPES.2021.03940.

[26] Wu, S.—Li, H.—Liu, Y.—Lu, Y.—Wang, Z.—Liu, Y.: A Two-Stage Rolling Optimization Strategy for Park-Level Integrated Energy System Considering Multi-Energy Flexibility. International Journal of Electrical Power & Energy Systems, Vol. 145, 2023, Art. No. 108600, doi: 10.1016/j.ijepes.2022.108600.

[27] Yang, J.—Zhao, J.—Qiu, J.—Wen, F.: A Distribution Market Clearing Mechanism for Renewable Generation Units with Zero Marginal Costs. IEEE Transactions on Industrial Informatics, Vol. 15, 2019, No. 8, pp. 4775–4787, doi: 10.1109/TII.2019.2896346.

[28] Li, Z.—Wu, L.—Xu, Y.—Moazeni, S.—Tang, Z.: Multi-Stage Real-Time Operation of a Multi-Energy Microgrid with Electrical and Thermal Energy Storage Assets: A Data-Driven MPC-ADP Approach. IEEE Transactions on Smart Grid, Vol. 13, 2022, No. 1, pp. 213–226, doi: 10.1109/TSG.2021.3119972.

[29] You, X.—Li, H.—Lu, Y.—Wang, J.—Chen, Y.: Pricing Strategy for Multi-Microgrids Centralized Trading Considering Distribution Network Power Flow. Power System Technology, Vol. 46, 2022, No. 4, pp. 1297–1309, doi: 10.13335/j.1000-3673.pst.2021.0492 (in Chinese).

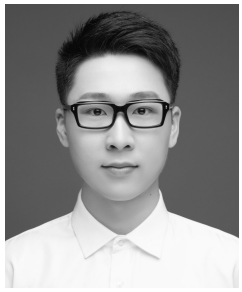

Yipeng Chen received his Bachelor degree from the Sichuan University, China, in 2021. He is currently a postgraduate student studying for the Master degree in the College of Electrical Engineering, Sichuan University, Chengdu, China. His research interests include integrated energy system operation, electricity market design and optimal optimization of power system.

Huaqiang Li received his Ph.D. degree in complex system engineering from the Hiroshima University, Japan, 2004. He is currently Professor in the College of Electrical Engineering, Sichuan University, Chengdu, China. He has authored over 100 papers and 2 books. He is now the Editor of the Power System Protection and Control. His research include security and stability of power system, planning and operation of power grid and microgrid, integrated energy system planning and operation.

Yang Liu received his Ph.D. degree in high-performance information retrieval from the Brunel University, U.K., in 2011. He is currently Associate Professor in the College of Electrical Engineering, Sichuan University, Chengdu, China. His research interests include renewable energy and energy storage technology, integrated energy system operation and high performance computing.

Shuning Wu received her Master degree from the Sichuan University, China in 2023. She will pursue her Ph.D. degree at the China Electric Power Research Institute, China. Her research interests include integrated energy system operation, multi-energy flexibility and optimal optimization of power system.

Xuan Li received his Master degree from the Sichuan University, China, in 2023. He will work in the State Grid Sichuan Technical Training Center. His research interests include energy storage technology, trading mechanism design.

Man Qi is Senior Lecturer in the Department of Computing at the Canterbury Christ Church University, U.K. Her research interests include cybercrime and computer forensics, intelligent computing, network application and human-computer interaction. She is a Fellow of the British Computer Society and also a Fellow of the Higher Education Academy.